



## Analysis of outdoor thermal discomfort over the Kingdom of Saudi Arabia

Item Type	Article
Authors	Dasari, Hari Prasad;Desamsetti, Srinivas;Langodan, Sabique;Vijaya Kumari, K.;Hoteit, Ibrahim
Citation	Dasari, H. P., Desamsetti, S., Langodan, S., Viswanadhapalli, Y., & Hoteit, I. (2021). Analysis of outdoor thermal discomfort over the Kingdom of Saudi Arabia. GeoHealth. doi:10.1029/2020gh000370
Eprint version	Post-print
DOI	<a href="https://doi.org/10.1029/2020gh000370">10.1029/2020gh000370</a>
Publisher	American Geophysical Union (AGU)
Journal	GeoHealth
Rights	Accepted manuscript version archived with thanks to GeoHealth.
Download date	2024-03-13 10:00:37
Link to Item	<a href="http://hdl.handle.net/10754/668892">http://hdl.handle.net/10754/668892</a>

## Analysis of outdoor thermal discomfort over the Kingdom of Saudi Arabia

Hari Prasad Dasari<sup>1</sup>, Srinivas Desamsetti<sup>1,2</sup>, Sabique Langodan<sup>1</sup>, Yesubabu Viswanadhapalli<sup>3</sup>,  
Ibrahim Hoteit<sup>1,\*</sup>

<sup>1</sup>*Physical Science and Engineering Division, King Abdullah University of Science and Technology,  
Kingdom of Saudi Arabia*

<sup>2</sup>*National Center for Medium Range Weather Forecasting (NCMRWF), Noida, India*

<sup>3</sup>*National Atmospheric Research Laboratory, Gadanki, India*

### Highlights:

- Analyze and investigate variability and trends of the outdoor thermal discomfort index (DI) in the Kingdom of Saudi Arabia (KSA).
- Reduced rate of increase in DI was reported in the southwestern region during the last 20 years.
- During this period, except Yanbu, Makkah, Madina, and Taif, most cities had an improved DI

### \*Corresponding author:

Prof. Ibrahim Hoteit,  
King Abdullah University of Science and Technology (KAUST),  
Thuwal 23955-6900, Saudi Arabia.  
E-mail: [ibrahim.hoteit@kaust.edu.sa](mailto:ibrahim.hoteit@kaust.edu.sa)

This article has been accepted for publication and undergone full peer review but has not been through the copyediting, typesetting, pagination and proofreading process, which may lead to differences between this version and the [Version of Record](#). Please cite this article as [doi: 10.1029/2020GH000370](#).

This article is protected by copyright. All rights reserved.

## Abstract

In this study, the variability and trends of the outdoor thermal discomfort index (DI) in the Kingdom of Saudi Arabia (KSA) were analyzed over the 39-year period of 1980–2018. The hourly DI was estimated based on air temperature and relative humidity data obtained from the next-generation global reanalysis from the European Center for Medium-Range Weather Forecasts and in-house high-resolution regional reanalysis generated using an assimilative Weather Research Forecast (WRF) model.

The DI exceeds 28°C, i.e., the threshold for human discomfort, in all summer months (June–September) over most parts of the KSA due to a combination of consistently high temperatures and relative humidity. The DI is greater than 28°C for 8–16 hours over the western parts of KSA and north of the central Red Sea. A DI of > 28°C persists for 7–9 hours over the Red Sea and western KSA for 90% of summer days. The spatial extent and number of days with DI > 30°C, i.e., the threshold for severe human discomfort, are significantly lower than those with DI > 28°C. Long-term trends in the number of days with DI > 28°C indicate a reduced rate of increase or even a decrease over some parts of the southwestern KSA in recent decades (1999–2018). Areas with DI > 30°C, in particular the northwestern regions of the Arabian Gulf and its adjoining regions, also showed improved comfort levels during recent decades. Significant increases in population and urbanization have been reported throughout the KSA during the study period. Analysis of five-years clinical data suggests a positive correlation between higher temperatures and humidity with heat-related deaths during the Hajj pilgrimage.

The information provided herein is expected to aid national authorities and policymakers in developing necessary strategies to mitigate the exposure of humans to high levels of thermal discomfort in the KSA.

**Keywords:** Kingdom of Saudi Arabia, Regional reanalysis, Discomfort index, Variability, Trends

## 1. Introduction

Climate change due to global warming has numerous effects on the living conditions of humans. Rising temperatures and the impact of urbanization result in heat stress and heat-related mortality (Kleerekoper et al., 2012). In the Kingdom of Saudi Arabia (KSA), changes in weather patterns and a sharp increase in extreme weather events are among the most significant drivers of social vulnerability, considerably threatening the living conditions of humans (Abdul Salam et al., 2014). Rapid growth in urbanization during recent decades and the consequent increase in impermeable surfaces of urban infrastructure surfaces have significantly changed urban ecosystems, substantially impacting the quality of life of urban residents (e.g., Ren et al., 2008; Warburton et al., 2012; Zhong et al., 2015; Du et al., 2019; Luong et al., 2020). The ability of urban dwellers to adapt to varying thermal environments largely depends on the external meteorological conditions. However, considering temperature variations alone may not provide a comprehensive picture of the threats posed by heat stress; ambient relative humidity must also be considered as it influences the evaporation of sweat, which helps to naturally maintain human comfort levels (Qaid et al., 2016; Huang et al., 2020). Air temperatures between 18°C and 23°C and relative humidity (RH) levels between 35% and 70% are considered to be the comfortable ranges for livability (Hoppe, 1999; Lin et al., 2010). However, these comfortable ranges may vary depending on the outdoor weather conditions and differ among residents from different climatic regions. When the human body is exposed to extreme heat and humidity, its cooling mechanisms, e.g., increased heart rate and sweating, are triggered (Cheong et al., 2017); these mechanisms can cause discomfort, weakness, loss of stamina, and muscle pains and, in severe cases, even heat strokes and heart attacks (Cheong et al., 2017).

The outdoor discomfort index (DI, expressed in units of °C) is a measure of the human heat sensation under different climatic conditions. The DI is computed using temperature and relative humidity, and it represents a quantitative assessment of stress due to heat. The DP helps evaluate how particular atmospheric conditions can affect the sensation of discomfort and the corresponding health risks to the population (e.g., Tom, 1959; Freitas and Grigorieva, 2015; Roghanchi and Kocsis, 2018). To consider cloudy conditions and their effects on longwave radiation scattering, several studies proposed using radiant temperature instead of air temperature when computing DI (e.g., Koch, 1962; Fanger, 1970; Gan, 2001). However, a lack of radiant temperature data for most regions hinders the use of this parameter in assessing human thermal stress (e.g., Gan, 2001; Ali-Toudert, 2005). In the case of KSA, the radiant temperature need not be used to estimation of the thermal comfort because of the prevalence of clear sky conditions and hot and dry climate throughout the year (Ali-Toudert, 2005). Hence, the DI may be computed based on temperature and relative humidity for this region (Anderson et al., 2013; Petitti et al., 2016).

Anderson et al. (2013) computed a heat stress index over several cities in the United States of America (USA) using 21 different methods and reported that calculating the DI based on temperature and humidity is the most robust and more suitable for regions with high temperatures. In other studies, the human health risk factor was calculated by measuring the combined effects of high ambient temperatures and humidity based on the simplified wet-bulb temperature and coarser resolution global datasets (e.g., Fischer and Knutti, 2013; Dunne et al., 2013; Zhao et al., 2015; Pal and Eltahir, 2016). Petitti et al. (2016) computed the DI over the state of Arizona, USA, using temperature and humidity in order to examine the relationship of DI with the mortality and hospitalization. A similar long-term assessment of the DI for the hot and humid climate of the

KSA can reveal the effects of thermal stress on the population and the variability of this stress with changes in the climatic conditions and the environment (e.g., urbanization). Such a comprehensive study detailing the variability and trends of DI derived from a reliable long-term, high-resolution dataset is still lacking for the KSA.

In most previous studies, the DI was examined using either the Intergovernmental Panel on Climate Change (IPCC) global climate model projections or regional models driven by the global climate models for various regions around the world. Despite the uncertainties associated with the IPCC projections and issues inherent to their downscaling, extreme wet-bulb temperatures projected for the future were suggested to approach and exceed the critical threshold values over the Arabian Gulf and its adjoining regions, which will severely impact human livability (Pal and Eltahir, 2016). Al-Bouwarthan et al. (2019) recently assessed the heat stress over the southeastern KSA during the summer of 2016 using a wet-bulb global temperature index and a temperature–humidity index, suggesting that the temperature–humidity index is the most suitable for evaluating heat stress risks over the KSA.

The objective of the present study is to describe, for the first time, to the best of our knowledge, the DI variability over the KSA based on an in-house atmospheric reanalysis data generated by using an assimilative Weather Research Forecast (WRF) model (Skamarock et al., 2019) over a 39-year period of 1980–2018. This extensively validated reanalysis of the KSA comprises unique information on the long-term weather conditions with a 5-km horizontal resolution grid and hourly intervals over the KSA. We computed the DI at every grid point across the entire study period and assessed its variability over hourly, seasonal, and interannual time scales. In addition, we performed a trend analysis to assess changes in the persistence of DI over time for different regions of the KSA and investigate possible relationships between this trend and

changes in population and urbanization. Furthermore, we attempted to establish a link between the available health-related data and changes in DI. The DI and associated trends were also computed using the European Center for Medium-Range Weather Forecasts (ECMWF) next-generation reanalysis (ERA, C3S, 2017) data for comparison.

The rest of this paper is organized as follows. The methodology for computing DI and the details of the analysed datasets are presented in Section 2. The results of the DI analysis over the KSA are reported and discussed in Section 3. Finally, a summary and the conclusions of the study are provided in Section 4.

## **2 Data and methodology**

### ***2.1 Datasets***

We analyzed temperature and relative humidity at a height of 2-m as suggested by the World Meteorological Organization (WMO, 2008) using two different data sources. The 2-m height accounts for the influence of free air, sunshine, and wind, and thus minimizing the effect of grass surfaces, trees, buildings, and other obstructions on measurement instruments (WMO, 2008). The first dataset is the ERA global reanalysis (C3S, 2017), available at ~15 km horizontal resolution and for every hour; this dataset has been widely used by the research community for several climate studies over the Arabian Peninsula (AP). The second dataset is an in-house regional high-resolution reanalysis that was specifically generated to study the climate of the AP using a WRF model assimilating all available regional observations (e.g., Viswanadhapalli et al., 2017, 2019a; Dasari et al., 2019; Sanjeev et al., 2020; Hoteit et al., 2021). The WRF was configured with 5 km/1 hour horizontal/temporal resolutions and used the ECMWF (ERA-Interim) fields as the boundary and initial conditions. This AP reanalysis has been extensively validated using *in situ* and remote sensing observations; additionally, it has been used in several studies (e.g., Viswanadhapalli et al.,

2017, 2019a, 2019b; Dasari et al., 2019; Langodan et al., 2016, 2020; Sanjeev et al., 2020; Hoteit et al., 2021); these studies provide the complete details regarding the methodology used to generate the AP reanalysis and describes its use for studying the regional climate variability and atmospheric and oceanic processes across the AP.

## ***2.2 Computation of outdoor thermal DI***

We estimated the DI based on temperature and relative humidity, as suggested by Thom (1959). This DI was used as an indicator for the heat stress on humans in several previous studies (e.g., Giles et al., 1990; Anderson et al., 2013; Freitas and Grigorieva, 2015; Roghanchi and Kocsis, 2018; Yasmeen and Liu, 2019). The DI (in °C) is computed as a function of air temperature (T; °C) and relative humidity (RH; %) as follows:

$$DI = T - 0.05(1 - 0.01RH)(T - 14.5).-----(1)$$

High DI indicate a high level of thermal human discomfort in humans. The suggested limits of DI according to previous studies (e.g., Marina et al., 2005; Anderson et al., 2013; Mishra et al., 2013, 2016; Nedel et al., 2015; Yasmeen and Liu, 2019) are classified in Table 1.

Herein, we computed the DI using ERA and WRF reanalysis data obtained over the summer months, i.e., from June–September (JJAS). We selected these months because of both their extreme heat and the significant changes in summer temperatures reported over the study region during the last few decades (e.g., Attada et al., 2018a; b; 2020). We categorized the estimated DI values based on the standard limits (Table 1), and thereafter, we explored its variability and trends over the past four decades.

### 3 Results

Human DI levels are closely related to the local temperature and relative humidity (RH) conditions. Therefore, we first analyzed the mean and maximum distributions of temperature and RH from both global and regional reanalyses. We also analyzed the changes in population and urbanization throughout the KSA. Subsequently, we examined the computed DI values to assess differences in their persistence and variability. Finally, we analysed the short-term and inter-decadal trends of DI.

#### *3.1 Analysis of mean temperature, relative humidity, population, and urbanization*

First, we analyzed the monthly mean (Figure 1) and maximum (Figure 2) temperatures and the monthly mean of RH (Figure 3) during summer using both ERA and AP reanalyses for the period of 1980–2018. The monthly mean temperature (Figure 1) in July and August are markedly higher than those in June and September. High temperatures are recorded throughout the summer, mainly over the northern KSA and the region extending from Kuwait to Oman. A significant east–west gradient of approximately 6°C –8°C exists over the KSA, with significantly higher temperatures near the Arabian Gulf compared with the Red Sea. Maximum daily temperatures (Figure 2) follow the same distribution as the mean daily temperatures in all four summer months, albeit with a considerably higher (~10°C –12°C) east–west gradient over the KSA. Although ERA and AP reanalyses indicate similar mean temperature patterns, the regional reanalysis temperatures exhibit higher values by approximately 1°C in the northwestern coastal regions of the KSA.

The mean monthly RH (Figure 3) exhibits a different distribution between the coastal and inland regions of the KSA. Higher RH values (more than 80%) dominate over the Red Sea, the Arabian Gulf, and other coastal areas, whereas inland regions experience arid conditions with RH values below 25%. The driest regions (RH < 10%–15 %) are located in the central KSA, most

significantly in June, following which the RH gradually decreases as the summer progresses; this decrease in RH occurs in conjunction with moisture transport from the Indian summer monsoon (Viswanadhapalli et al., 2017; Attada et al., 2018b). Good agreement between the ERA and the regional AP reanalyses confirms that the latter accurately reproduces the large-scale patterns of temperature and RH over the KSA.

Environmental conditions, such as temperature and RH, are critical in determining a region's livability (Pal and Eltahir, 2016; Al Mayahi, 2019; Liang et al., 2020). Considering this, we analyzed population hot spots with vulnerable living conditions in the KSA. The KSA has 13 administrative divisions (Figure 4a), all of which witnessed a consistent increase in population since 1980 (Figure 4b). Of these 13 regions, seven have more than 1 million inhabitants (Figure 4c); Al-Riyadh and Makkah are the most populated regions with more than 6 million inhabitants each, followed by Ash Sharqiyah with approximately 4 million inhabitants, and Madinah, Qassim, Asir, and Jizan with around 1–2 million inhabitants each. Census reports (Census, 2010) indicates a significant increase in population (by about 30%) between 1992 and 2010 in all administrative regions (Figure 4b). This sharp increase in population has promoted rapid urbanization (Lowry, 1991; Carrol, 2007). Indeed, the urban canopy, which is a measure of urbanization, indicates a substantial extension of nearly two- to three-fold in major cities of the KSA (Figure 5). Most recently, Alahmadi et al. (2019) reported a three-fold increase in urban morphology based on satellite images, mainly over Al-Riyadh, Makkah, and Eastern administrative regions, between 1992 and 2013. They further reported a 30% growth in urbanization during 1999–2006, which increased to 55% during 2006–2013, suggesting a significant increase in urbanization in the KSA in recent years.

Additionally, several million people visit the KSA annually to perform the Hajj pilgrimage. The Hajj season follows the lunar calendar, and between 2014 and 2018, it occurred in the summer months (June–September), when the average temperature and humidity often exceeds 40°C and 80%, respectively (National Hajj Extreme Heat Strategy, 2016). Such high temperatures and humidity increase the heat stress and may cause health issues. For example, the number of heatstroke and heat exhaustion cases reported in each year in five different regions (Makkah, Madinah, Mena, Arafat, and Mozdalifah) during the Hajj period (Table 2) clearly indicate a correlation between the heat exhaustion cases and the high temperatures and humidity. Based on clinical data during the 2016 Hajj season, Abdelmoety et al. (2018) reported that ~29% and ~67.7% of the total cases admitted to hospitals were due to heat stroke and heat exhaustion, respectively, with 6.3% and 0.0% mortality, respectively.

Several studies have also reported that construction workers in the KSA are increasingly susceptible to critical health effects owing to heat exposure (e.g., Inaba and Mirbod, 2007; Horie, 2013; Jia et al., 2016; El-Shafei et al., 2018). These effects include chronic health problems such as psychological distress (e.g., Smith et al., 1997; Tawatsupa et al., 2010), and cardiovascular (e.g., Vangelova et al., 2006) and kidney diseases (e.g., Tawatsupa et al., 2012; Luo et al., 2014). Therefore, analyzing the long-term DI and its variability and trends in relation to the rapid urbanization and increasing population of the KSA is crucial.

### ***3.2 Analysis of the mean DI***

The monthly mean DI values as computed from ERA and AP reanalyses using equation (1) for the summer months are presented in Figure 6. The mean spatial patterns from both datasets indicate that the DI exceeds 29°C over most parts of the western KSA and the Red Sea regions. The highest values are recorded in July and August over the Arabian Gulf, probably because of the Shamal

winds, which reach their maximum strength during these months (Viswanadhapalli et al., 2019a). These winds transport heat and moisture towards the AP. The entire east coast of the Red Sea, extending from the northwest to the southwest of the KSA, exhibits relatively lower DI values ( $\sim 22^{\circ}\text{C}$ – $29^{\circ}\text{C}$ ) compared with other regions in the KSA.

The mean number of hours per day with  $\text{DI} > 28^{\circ}\text{C}$  and  $\text{DI} > 30^{\circ}\text{C}$  are shown in Figures 7 and 8, respectively. The results obtained from both ERA and AP reanalyses suggest that  $\text{DI} > 28^{\circ}\text{C}$  persists for around 8–10 hours per day over the western KSA and about 14–16 hours per day over Oman and the adjoining regions (Figure 7). The number of hours per day with  $\text{DI} > 28^{\circ}\text{C}$  is relatively consistent over the western KSA throughout the summer, and it spatially extends during July and August. The southern Red Sea and the Arabian Gulf experience  $\text{DI} > 28^{\circ}\text{C}$  for about 14–16 hours per day.

The mean number of hours per day with  $\text{DI} > 30^{\circ}\text{C}$  is shown in Figure 8. These results suggest that the Arabian Gulf experiences  $\text{DI} > 30^{\circ}\text{C}$  for about 6–8 hours per day. The areal extent of  $\text{DI} > 30^{\circ}\text{C}$  for 6–8 hours per day is larger over the northwest part of the KSA and adjoining countries; this extent may be related to the clear sky conditions over this region (Kunchala et al., 2018; 2019; Gandham et al., 2020; Dasari et al., 2019; 2020), as well as the dominant land use and vegetation coverage (Gandham et al., 2020). The eastern region of the KSA mainly comprises arid land with highly urbanized areas characterized by a higher specific heat capacity than the moderately vegetated hilly regions of the western KSA. The southern Red Sea coast of Sudan and the Arabian Gulf experience  $\text{DI} > 30^{\circ}\text{C}$  for  $\sim 8$ –14 hours per day during July and August, indicating a severe level of human discomfort during these months. The high DI in this region may be associated with the channeling of the Indian summer monsoon winds and the associated transport of moisture, resulting in increased humidity, and subsequently, a high DI.

We further computed the mean number of days during which  $DI > 28^{\circ}\text{C}$  persisted for 4–6 hours and 7–9 hours per day for each summer month using the global and regional reanalyses (Figures S1 and S2). The corresponding results are presented and discussed in the Supplementary Material; these results provide information on the spatial patterns of the number of days with persistently high DI, and it can help policy makers in various sectors to adopt necessary precautionary measures related to business hours, health conditions, energy balance, and heat stress, among other factors.

The mean number of days during which  $DI > 28^{\circ}\text{C}$  persists for 4–6 hours and 7–9 hours per day for each month in the major cities of the KSA are listed in Table 3. The results indicate that the number of days with  $DI > 28^{\circ}\text{C}$  is greatly lower for the cities located in the central KSA region, including Makkah, Madina and Taif. The number of days with  $DI > 28^{\circ}\text{C}$  is relatively higher (lower) over Jeddah and Yanbu provinces than over the central (eastern) cities. The maximum number of days with  $DI > 28^{\circ}\text{C}$  were recorded over the eastern parts of KSA, in the Al-Riyadh, Al-Hofuf, Dammam, and Al Jubail provinces.

The above climatological analysis of the distribution of  $DI > 28^{\circ}\text{C}$  and  $DI > 30^{\circ}\text{C}$  indicates that the level of human thermal discomfort during summer is higher in the western KSA (i.e., the Arabian Gulf and its adjoining regions) and the southern Red Sea than in the other regions of the KSA. Further, the human thermal discomfort in the southeast regions of the KSA and its adjoining countries, including the United Arab Emirates (UAE), Oman, Bahrain, and Kuwait, is higher than that in the northern and northwestern regions of the KSA.

### ***3.3 Changes in the DI during 1980–2018***

To assess changes in human thermal discomfort throughout the KSA during the past four decades, i.e., 1980–2018, we analyzed the linear trends with a 95% confidence level over the entire study

period and for different sub-periods therein. We computed the linear trends for the number of hours per day with  $DI > 28^{\circ}\text{C}$  and  $DI > 30^{\circ}\text{C}$  at every grid point, and obtained the results at the 95% confidence level based on a Student's t-test (Panofsky and Brier, 1968). To identify recent changes in DI compared to the DI in past four decades, and to further understand the recent changes influencing human thermal discomfort, we divided the study period (1980–2018) into two subperiods: the past, i.e., 1980–1998 and the recent, i.e., 1999–2018 periods. The year 1998 was selected for demarcation is based on previous studies that reported drastic changes in the Walker and Hadley circulation around this time as a result of the mega El-Nino Southern Oscillation (ENSO) event during that year (Wang et al., 2012; 2013). Furthermore, the KSA has witnessed significant industrialization since 1998 (Belloumi and Alshehry, 2016). Therefore, we expect urban areas, which have developed together with industrialization, to be more adversely affected in terms of human thermal comfort in the recent decades. Herein, we present only the trend analysis for the DI derived from the regional AP reanalysis for the major populated regions of KSA (shown in Figure 5). The spatial distributions of DI trends from both the AP and ERA reanalyses are provided in the Supplementary Material (Figures S2–S7).

The trends of the mean number of days in summer with  $DI > 28^{\circ}\text{C}$  persisting for 4–6 hours per day over the major cities of the KSA are shown in Figure 9. The trends (days/decade) for the individual months are listed in Table 4. The mean number of days with thermal discomfort significantly increased (at the 95% confidence level) during recent decades in Taif, Makkah, Madina and Yanbu, suggesting a significant deterioration in the thermal discomfort during the latest two decades in all four summer months. The other cities showed an increase at the 95% confidence level during the 1980–1998 period followed by a nonsignificant decrease in the 1999–2018 period. Makkah and Madina experienced a slight decrease in the number of days with  $DI >$

28°C persisting for 4–6 hours per day in September, and a significant increase in June, July, and August during the recent decades. These results clearly suggest that the levels of outdoor thermal discomfort have improved over most of the major cities of the KSA during the recent decades, with the exception of high-altitude cities, such as Makkah, Madina, and Taif, where the DI has deteriorated over time. Although these cities exhibited relatively small number of days with  $DI > 28^{\circ}\text{C}$  persisting for 4–6 or 7–8 hours per day (Table 3) before 1998, this number has significantly increased (at the 95% confidence level) throughout the recent decades.

#### **4 Summary and conclusions**

Herein, we analyzed the discomfort index (DI), which is a measure of outdoor thermal discomfort, during the summer months (i.e., June–September) across the KSA between 1980 and 2018. The DI was computed based on temperature and relative humidity (RH) data from two independent data sources: a regional atmospheric reanalysis generated using an assimilative WRF model configured with 5-km horizontal resolution and the global reanalysis ERA. We conducted detailed comparisons of the estimated DI values to confirm their consistency. The DI time series computed at every grid point over the entire study period were analyzed to investigate the variability and associated trends at different time-scales throughout the KSA.

The analysis results suggest that the majority regions across the KSA experienced  $DI > 28^{\circ}\text{C}$  in summer (i.e., June–September), which is associated with high surface temperatures and RH.  $DI > 28^{\circ}\text{C}$ , a condition at which most people experience discomfort, persisted for ~8–16 hours per day over the KSA throughout the summer months. We found that on around 90% of the total summer days,  $DI > 28^{\circ}\text{C}$  persisted for 7–9 hours per day over the Red Sea and western KSA during all four months. We also detected similar spatial patterns and trends for  $DI > 30^{\circ}\text{C}$ , which is an

indicator of extreme human discomfort. These higher DI values were mainly concentrated over the neighboring regions of the Arabian Gulf and some parts of the southern Red Sea.

The trend analyses of  $DI > 28^{\circ}\text{C}$  and  $30^{\circ}\text{C}$  revealed a significant improvement in the human thermal discomfort in recent decades over the southern Red Sea, some parts of the northwestern Arabian Gulf, and their adjoining regions. The results revealed a reduced rate of increase, or even a decrease in the number of days with a persistently high DI for these regions in the last twenty years (i.e., 1999–2018). In contrast, human thermal discomfort over the southeast regions of the KSA, UAE, Oman, and Qatar have exhibited a positive trend in recent decades. Changes in DI over recent decades can be attributed to variations in meteorological and/or microclimatic conditions, and requires further detailed analysis.

Knowledge of the variability and trends of outdoor thermal discomfort over the KSA will provide a reference for policy makers and urban planners. The development of a comprehensive understanding of the region's climatology and its effects on the long-term trends of DI enables authorities to determine which regions of the KSA are and may remain comfortable for the population in the future. Additionally, it will also provide engineers with important information for designing efficient infrastructure with effective ventilation and cooling capacity by updating the existing protocols to meet adequate conditions for the safety, health, and comfort of the population. Detailed knowledge of the DI is further critically important for supporting the ongoing developments of several large-scale projects that are being developed in the KSA, e.g., NEOM (<https://www.neom.com>), the Red Sea Project (<https://www.theredsea.sa>), and AMAALA (<https://www.amaala.com/en/home>), among others, providing crucial information about the regional environment for optimizing the design and the operations of these new developments. The framework developed herein is a stepping-stone toward developing a forecasting system that

could provide important information for outdoor and sports activities, energy consumption management, military planning, tourism, the mining industry, street vendors, and outdoor workers, among many other parties.

### **Acknowledgments:**

This work was supported by the office of Sponsor Research (OSR) at King Abdullah University of Science and Technology (KAUST) under the Virtual Red Sea Initiative (REP/1/3268-01-01) and the Saudi ARAMCO-KAUST Marine Environmental Observatory (SAKMEO). This research utilized the Supercomputing Laboratory resources at KAUST. The datasets of the European Center for Medium-Range Weather Forecasts (ECMWF's) next-generation reanalysis (C3S, 2017), Saudi Arabia population data (Census, 2010), and clinical data reported during Hajj (National Hajj Extreme Heat Strategy, 2016) are freely available and properly cited in the manuscript. All remaining datasets used in this study are deposited, under GeoHealth FAIR data policy, at [https://figshare.com/articles/dataset/Datasets\\_for\\_the\\_GeoHealth\\_2020GH000370/14388170](https://figshare.com/articles/dataset/Datasets_for_the_GeoHealth_2020GH000370/14388170).

The authors would like to thank the anonymous reviewers for their constructive and valuable comments.

### **References**

1. Abdelmoety, D.A., El-Bakri, N.K., Almowalld, W.O., Turkistani, Z.A., Bugis, B.H., Baseif, E.A., Melbari, M.H., AlHarbi, K., Abu-Shaheen, A., 2018. Characteristics of heat illness during Hajj: a cross-sectional study. *BioMed Res. Int*, 5629474, doi: 10.1155/2018/5629474.

- Accepted Article
2. Abdul Salam, A., Elsegaey, I., Khraif, R., Al-Mutairi, A., 2014. Population distribution and household conditions in Saudi Arabia: reflections from the 2010 Census. SpringerPlus, 3, 530.
  3. Al Mayahi, Z.K., Ali Kabbash, I., 2019. Perceptions of, and practices for coping with, heat exposure among male Arab pilgrims to the Hajj, 1436. Prehosp. Disaster Med., 34, 161–174.
  4. Al-Bouwarthan, M., Quinn, M.M., Kriebel, D., Wegman, D.H. 2019. Assessment of heat stress exposure among construction workers in the hot desert climate of Saudi Arabia. Ann. Work Expo. Health., 63, 505–520.
  5. Alahmadi, M., Atkinson, P.M., 2019. Three-fold urban expansion in Saudi Arabia from 1992 to 2013 observed using calibrated DMSP-OLS night-time lights imagery. Remote Sens., 11(19), 2266.
  6. Ali-Toudert F., 2005. Dependence of the outdoor thermal comfort on street design in hot and dry climate. Berichte des Meteorologischen Institutes der Universität, Freiburg., 15, 1–229.
  7. Anderson, G.B., Bell, M.L., Peng, R.D., 2013. Methods to calculate the heat index as an exposure metric in environmental health research. Environ. Health Perspect., 121, 1111–1119
  8. Aneesh, S., Sijikumar, S., 2016. Changes in the south Asian monsoon low level jet during recent decades and its role in the monsoon water cycle. J. Atmos. Sol.-Terr. Phys., 139, 47–53.

9. Attada, R., Dasari, HP., Chowdary, JS., Ramesh Kumar, Y., Knio, O., Hoteit, I., 2018a. Surface air temperature variability over the Arabian Peninsula and its links to circulation Patterns. *Int J Climatol.*, 39, 445–464, DOI:10.1002/joc.5821.
10. Attada, R., Dasari, HP., Kunchala, RK., L. Sabique., Ramesh Kumar, Y., Niranjan Kumar, K., Knio, O., Hoteit, I., 2020. Evaluating cumulus parameterization schemes for the simulation of Arabian Peninsula winter rainfall. *J. of Hydrometeorology.*, 21, 5, 1089–1114.
11. Attada, R., Kunchala, RK., Ramesh Kumar, Y., Dasari, HP., Knio, O., Hoteit, I., 2018b. Prominent modes of summer surface air temperature variability and associated circulation anomalies over the Arabian Peninsula. *Atmos. Sci. Lett.*, 19, e860, <https://doi.org/10.1002/asl.860>.
12. Belloumi, M., Alshehry, AS., 2016. The impact of urbanization on energy intensity in Saudi Arabia. *Sustainability*, 8(4), 375.
13. Carroll, W. K., 2007. Global Cities in the Global Corporate Network. *Environ. Plan A.*, 39(10): 2297–2323.
14. Census, 2010. Saudi Census, General Authority for Statistics, Kingdom of Saudi Arabia, <https://www.stats.gov.sa/en/73> (Accessed on 5 August 2020).
15. Cheong et al., 2017. IEEE 9th International Conference on Humanoid, Nanotechnology, Information Technology, Communication and Control, Environment and Management (HNICEM). Proceedings of HNICEM held on 1-3 December 2017, Manila, Philippines. ISBN: 9781538609132, Vol.1, pages 798.

16. Copernicus Climate Change Service (C3S)., 2017. ERA5: Fifth generation of ECMWF atmospheric reanalyses of the global climate. Copernicus Climate Change Service Climate Data Store (CDS), doi:10.24381/cds.adbb2d47 (accessed on 04 December 2019).
17. Dasari, HP., Desamsetti, S., L. Sabique., Attada, R., Viswanadhapalli, Y., Kunchala, RK., Hoteit, I., 2019: Assessment of solar radiation resources and its variability over Arabian Peninsula. *Appl. Energy*, 248, 354–371.
18. Dasari, HP., Desamsetti, S., L. Sabique., Karumuri, R., Singh, S., Hoteit, I., 2020: Atmospheric conditions and air quality assessment over NEOM, Kingdom of Saudi Arabia. *Atmos. Environ.*, 117489. <https://doi.org/10.1016/j.atmosenv.2020.117489>.
19. Du, J., Cheng, L., Zhang, Q., Yang, Y., and Xu, W., 2019. Different flooding behaviors due to varied urbanization levels within river basin: A case study from the Xiang River basin, China. *Int. J. Disaster Risk Sci*, 10, 89–102.
20. Dunne, JP., Stouffer, RJ., John, JG., 2013. Reductions in labour capacity from heat stress under climate warming. *Nat. Clim. Change*, 3, 563–566
21. El-Shafei, D.A., Bolbol, S.A., Awad Allah. M.B., et al., 2018. Exertional heat illness: knowledge and behavior among construction workers. *Environ. Sci. Pollut. Res. Int*, 25, 32269–32276.
22. Fanger, P.O., 1970., Thermal comfort: analysis and applications in environmental engineering. New York: McGraw Hill. 244 pages. ISBN: 8757103410, 9788757103410.
23. Fischer, EM., Knutti, R., 2013. Robust projections of combined humidity and temperature extremes, *Nat. Clim. Change*, 3, 126–30.
24. Freitas, CR., Grigorieva, EA., 2015. A comprehensive catalogue and classification of human thermal climate indices. *Int. J. Biometeorol.*, 59, 109–120.

25. Gan G., 2001. Analysis of mean radiant temperature and thermal comfort. *Build. Serv. Eng. Res. Technol.*, 22(2), 95–101.
26. Giles, B., Balafoutis C. and Maheras, P. 1990. Too hot for comfort: The heat waves in Greece in 1987 and 1988. *Intern. J. Biometeorol.*, 34(2), 98 –104.
27. Höppe, P., 1999. The physiological equivalent temperature-a universal index for the biometeorological assessment of the thermal environment. *Int. J. Biometeorol.*, 43, 71–75.
28. Horie S., 2013. Prevention of heat stress disorders in the workplace. *J. Jpn. Med. Assoc.*, 56, 186–92.
29. Hoteit et al., 2021. Towards an end-to-end analysis and prediction system for weather, climate, and marine applications in the Red Sea. *Bull. Amer. Met. Soc.*, E99–E122, <https://doi.org/10.1175/BAMS-D-19-0005.1>
30. Huang, C.-H., Tsai, H.-H., Chen, H.-C., 2020. Influence of weather factors on thermal comfort in subtropical urban environments. *Sustainability*, 12, 2001, <https://doi.org/10.3390/su12052001>.
31. Inaba, R., Mirbod, S.M., 2007. Comparison of subjective symptoms and hot prevention measures in summer between traffic control workers and construction workers in Japan. *Ind. Health*, 45, 91–99.
32. Jia, Y.A., Rowlinson, S., Ciccarelli, M., 2016. Climatic and psychosocial risks of heat illness incidents on construction site. *Appl. Ergon.*, 53, 25–35.
33. Kleerekoper L, Van Esch M, Salcedo TB., 2012. How to make a city climate-proof, Addressing the urban heat island effect. *Resour. Conserv. Recycl.*, 64, 30–38.
34. Koch, W., 1962. Relationship between air temperature and mean radiant temperature in thermal comfort. *Nature*, 196, 587.

35. Kunchala, RK., Attada, R., Dasari, HP., Ramesh Kumar, V., L. Sabique., Yasser, A., Hoteit, I., 2018. Aerosol Optical Depth Variability over the Arabian Peninsula inferred from satellite measurements. *Atmos. Environ.*, 187, 346–357.
36. Kunchala, RK., Attada, R., Dasari, HP., Ramesh, K., Yasser, A., Ashok, K., Hoteit, I., 2019: On the Recent Amplification of Dust over the Arabian Peninsula during 2002 to 2012. *J. Geophys. Res. Atmos.*, 124(23), 13220–13229.
37. Gandham, H., Dasari, H., Langodan, S., RamaKrishna, K., Hoteit, I., 2020. Major changes in extreme dust events dynamics over the Arabian Peninsula during 2003–2017 driven by atmospheric conditions. *J. Geophys. Res. Atmos.*, 125, 24, doi:10.1029/2020JD032931.
38. Langodan, S., A. Charls., P. Shanas., Dasari, HP., Yasser, A., Hoteit, I., 2020: Wave modelling of a reef sheltered coastal zone in the Red Sea. *Ocean Eng.*, 207, 107378, doi:<https://doi.org/10.1016/j.oceaneng.2020.107378>
39. Langodan, S., Viswanadhapalli, Y., Dasari, HP., Knio, O., Hoteit, I., 2016. A high-resolution assessment of wind and wave energy potentials in the Red Sea. *Appl. Energy.*, 181, 244–255.
40. Liang, L., Deng, X., Wang, P., Wang, Z., Wang, L., 2020. Assessment of the impact of climate change on cities livability in China. *Sci. Total Environ.*, 726, 138339, doi: <https://doi.org/10.1016/j.scitotenv.2020.138339>
41. Lin, TP., Matzarakis, A., Hwang, RL., 2010. Shading effect on long-term outdoor thermal comfort. *Build. Environ.*, 45, 213–221.
42. Lowry, I. S., 1990. World urbanization in perspective. *Population and development review.* 16, 148–176, doi:<https://doi.org/10.2307/2808068>.

43. Lowry, Ira (1991). "World urbanization in perspective," In: Kingsley Davis and Mikhail Bernstam (eds.), *Resources, Environment and Population: Present Knowledge, Future Options*, (New York: Oxford University Press), pp. 148–176.
44. Luo, H., Turner, L.R., Hurst, C., et al. 2014. Exposure to ambient heat and urolithiasis among outdoor workers in Guangzhou, China. *Sci. Total Environ*, 472, 1130–1136.
45. Luong, TM., Dasari, HP., I. Hoteit, I., 2020: Impact of urbanization on the simulation of extreme rainfall in the city of Jeddah, Saudi Arabia. *J. Appl. Meteorol. Climatol.*, 59 (5), 953–971.
46. Marina, IS., Costas, C., Iphigenia, K., Mat, S., 2005. Thermal remote sensing of Thom's Discomfort Index (DI): Comparison with in situ measurements. *Proceedings of SPIE - The International Society for Optical Engineering*, 5983, 131–139, DOI:10.1117/12.627541.
47. Mishra, AK., Loomans, M., Hensen, J. 2016. Thermal comfort of heterogeneous and dynamic indoor conditions - an overview. *Build. Environ.*, 109, 82–100
48. Mishra, AK., Ramagopal, M., 2013. Field studies on human thermal comfort — An overview. *Build. Environ.*, 64, 94–106.
49. National Hajj Extreme Heat Strategy, 2016. Ministry of Health, Kingdom of Saudi Arabia. <https://www.moh.gov.sa/en/Hajj/PublicationsAwareness/Publications/Documents/National-Hajj-Extreme-Heat-Strategic-Strategy.pdf> (Accessed on 5 August 2020).
50. Nedel, AS., Gonçalves, FLT., Macedo-Junior, C., Cardoso, MRA., 2015. Climatology of the human thermal comfort on Sao Paulo metropolitan area, Brazil: indoors and outdoors. *Rev. Bras. Geofis.*, 33(2), 185–204.
51. Pal, JS., Eltahir, EAB., 2016. Future temperature in southwest Asia projected to exceed a threshold for human adaptability. *Nat. Clim. Change.*, 6, 197–200.

52. Panofsky HA, Brier GW., 1968. Some applications of statistics to meteorology, Pennsylvania State University, University Park; 224.
53. Petitti, D. B., Hondula, D.M., Yang S., Harlan, S.L., and Chowell. G., 2016. Multiple trigger points for quantifying heat-health impacts: new evidence from a hot climate *Environ. Health Perspect.*, 124 (2), 176–183.
54. Qaid, A., Bin Lamit, H., Ossen, D.R., Raja Shahminan, R.N., 2016. Urban heat island and thermal comfort conditions at micro-climate scale in a tropical planned city. *Energy Build*, 133, 577–595.
55. Ren, G., Y. Zhou, Z. Chu, J. Zhou, A. Zhang, J. Guo, and X. Liu., 2008. Urbanization effects on observed surface air temperature trends in north China. *J. Climate*, 21(6), 1333–1348.
56. Roghanchi, P., Kocsis, KC., 2018. Challenges in selecting an appropriate heat stress index to protect workers in hot and humid underground mines. *Safe. Health at Work*, 9(1), 10–16, <https://doi.org/10.1016/j.shaw.2017.04.002>.
57. Sanjeev, D., Viswanadhapalli, Y., Venkataratnam, M., Dasari, HP., L. Sabique., Raj, A., Hoteit, I., 2020. Variability of monsoon inversion over the Arabian Sea and its impact on rainfall. *Int. J. Climatol.*, 41(S1), E2979–E2999.
58. Skamarock, W. C., J. B. Klemp, J. Dudhia, D. O. Gill, Z. Liu, J. Berner, W. Wang, J. G. Powers, M. G. Duda, D. M. Barker, X.-Y. Huang., 2019. A description of the advanced research WRF Version 4. NCAR Tech. Note NCAR/TN-556+STR, 145 pp.
59. Smith, D.L., Petruzzello, S.J., Kramer, J.M., et al., 1997. The effects of different thermal environments on the physiological and psychological responses of firefighters to a training drill. *Ergonomics*, 40 (4), 500–510.

60. Tawatsupa, B., Lim, L.L., Kjellstrom, T., et al. 2010. The association between overall health, psychological distress, and occupational heat stress among a large national cohort of 40,913 Thai workers. *Glob. Health Action*, 3, 5034–5043.
61. Tawatsupa, B., Lim, L.L., Kjellstrom, T., et al. 2012. Thai Cohort Study Team. Association between occupational heat stress and kidney disease among 37,816 workers in the Thai cohort study (TCS). *J. Epidemiol.*, 22, 251–260.
62. Thom, E.C., 1959. The discomfort index. *Weatherwise*, 12, 57–60.
63. van Hove, LWA., Jacobs, CMJ., Heusinkveld, BG., Elbers, JA., van Driel, BL., Holtslag, AAM., 2015. Temporal and spatial variability of urban heat island and thermal comfort within the Rotterdam agglomeration. *Build. Environ.*, 83 (Suppl. C), 91–103.
64. Vangelova, K., Deyanov, C., Ivanova, M., 2006. Dyslipidemia in industrial workers in hot environments. *Cent. Eur. J. Public Health*, 14, 15–17.
65. Viswanadhapalli, Y., Challa, VS., Basha, G., Dasari, HP., Venkata Ratnam, M., L. Sabique., I. Hoteit., 2019b. A diagnostic study of extreme precipitation over Kerala during August 2018. *Atmos. Sci. Lett.*, 20 (12), e941, DOI: 10.1002/asl.94.
66. Viswanadhapalli, Y., Dasari, HP., Langodan, S., Srinivas, C.V., Hoteit, I., 2017. Climatic features of the Red Sea from a regional assimilative Model. *Int. J. Climatol.*, 37 (5), 2563–2581.
67. Viswanadhapalli, Y., Dasari, HP., Sanjeev, D., Venkata Ratnam, M., Langodan, S., Hoteit, I., 2019a. Variability of Monsoon Low Level Jet and associated rainfall over India. *Int. J. Climatol.*, 40 (2), 1067–1089.
68. Wang, B., Liu, J., Kim, HJ., Webster, PJ., Yim, SY., 2012. Recent changes of the global monsoon precipitation (1979–2008). *Clim. Dyn.*, 39(5), 1123–1135.

69. Wang, B., Liu, J., Kim, HJ., Webster, PJ., Yim, SY., Xiang B., 2013. Northern Hemisphere summer monsoon intensified by mega-El Niño/southern oscillation and Atlantic multidecadal oscillation. PNAS, 110 (14), 5347–5352.
70. Warburton, M.L., R.E. Schulze, and G.P.W. Jewitt., 2012. Hydrological impacts of land use change in three diverse South African catchments. J. Hydrology, 414, 118–135.
71. World Meteorological Organization, 2008. Guide to Meteorological Instruments and Methods of Observations, WMO No. 8, 1-681, ISBN: 978-92-63-100085, <https://www.weather.gov/media/epz/mesonet/CWOP-WMO8.pdf>
72. Yasmeen, S., Liu, H., 2019. Evaluation of thermal comfort and heat stress indices in different countries and regions – a review. IOP Conference Series: Materials Science and Engineering, Volume 609, (5). doi:10.1088/1757-899X/609/5/052037.
73. Zhao, Y., Ducharne, A., Sultan, B., Braconnot, P., Vautard, R., 2015. Estimating heat stress from climate-based indicators: present-day biases and future spreads in the CMIP5 global climate model ensemble. Env. Res. Letters., 10, 084013.
74. Zhong, S., Y. Qian, C. Zhao, R. Leung, and X.-Q. Yang., 2015. A case study of urbanization impact on summer precipitation in the Greater Beijing Metropolitan Area: Urban heat island versus aerosol effects. J. Geophys. Res. Atmos., 120(20), 10903–10914.

## Tables:

Table 1. Classification of human thermal discomfort based on the discomfort index (DI)

Sr. No	Human thermal discomfort classification	DI range (°C)
1	No discomfort	<21
2	Under 50% population feels discomfort	21 < DI < 24
3	Over 50% population feels discomfort	24 < DI < 27
4	Most of the population suffers discomfort	27 < DI < 29
5	Everyone feels severe discomfort	29 < DI < 32
6	State of medical emergency	DI > 32

Table 2: Total number of cases of heat stroke (heat exhaustion) cases reported in four different regions during the Hajj season.

Region	2014	2015	2016	2017	2018
Makkah	8 (7)	163 (38)	16 (15)	38 (15)	15 (17)
Madinah	1 (2)	2 (1)	3 (3)	0 (1)	0 (8)
Mena	57 (186)	324 (630)	70 (337)	170 (535)	130 (649)
Arafat and Mozdalifah	16 (214)	228 (345)	8 (171)	57 (180)	18 (187)
Total	82 (409)	717 (1014)	97 (526)	265 (731)	163 (861)

Source: Ministry of Health (2019).

Table 3: Mean number of days in each month in which  $DI > 28^{\circ}\text{C}$  persisting for 4–6 hours /day (7–9 hours/day) over the major cities of in the Kingdom of Saudi Arabia (KSA).

Urban regions	No. of days in which $DI > 28^{\circ}\text{C}$ persisted for 4–6 hours /day (7–9 hours/day)			
	June	July	August	September
Al-Riyadh	15 (8)	26 (15)	24 (16)	9 (6)
Al-Hofuf	16 (11)	26 (23)	25 (22)	11 (5)
Dammam	20 (11)	26 (22)	27 (23)	13 (8)
Al Jubail	15 (8)	24 (20)	25 (13)	12 (4)
Jeddah	10 (6)	16 (13)	17 (14)	14 (12)
Makkah	2 (1)	2 (1)	3 (1)	2 (1)
Taif	2 (1)	3 (1)	3 (1)	2 (1)
Madinah	2 (1)	3 (1)	2 (1)	2 (1)
Yanbu	12 (6)	13 (7)	16 (12)	11 (6)

Table 4: Trends of the number of days per decade with  $DI > 28^{\circ}\text{C}$  persisting for 4–6 hours per day over the major cities of the KSA. The number of days shown in shaded boxes indicate those with more than 95% confidence level.

Urban regions	Trends of the number of days for which $DI > 28^{\circ}\text{C}$ persisted for 4–6 hours/day											
	1980-2018				1980-1998				1999-2018			
	June	July	Aug	Sep	June	July	Aug	Sep	June	July	Aug	Sep
Al-Riyadh	2.5	2.25	2.1	2.0	2.1	–1.2	2.1	1.9	–0.4	–0.2	0.3	2.1
Al-Hofuf	0.9	0.2	0.4	1.2	1.7	–1.5	1.2	2.1	–0.6	0.1	–0.3	–0.5
Dammam	1.7	0.5	1.4	1.2	2.2	–0.8	2.3	0.1	–0.4	–0.1	–0.2	–0.1
Al Jubail	1.75	0.2	1.2	1.2	2.1	–0.8	0.2	0.4	–0.3	–0.2	–0.1	1.1
Jeddah	0.1	0.1	0.1	0.1	0.2	0.1	0.1	0.1	–0.1	–0.1	–0.1	–0.1
Makkah	0.6	1.5	1.2	0.6	0.7	0.3	1.3	–0.2	1.3	1.2	1.4	–0.2
Taif	1.6	1.9	1.8	0.5	1.7	0.6	1.9	0.4	1.6	1.8	1.1	1.1
Madinah	1.4	2.4	2.6	0.2	0.2	–0.7	2.8	–0.1	1.6	2.6	–0.5	–0.2
Yanbu	0.9	2.1	2.4	1.2	0.2	1.1	2.6	1.6	1.8	2.2	0.3	0.3

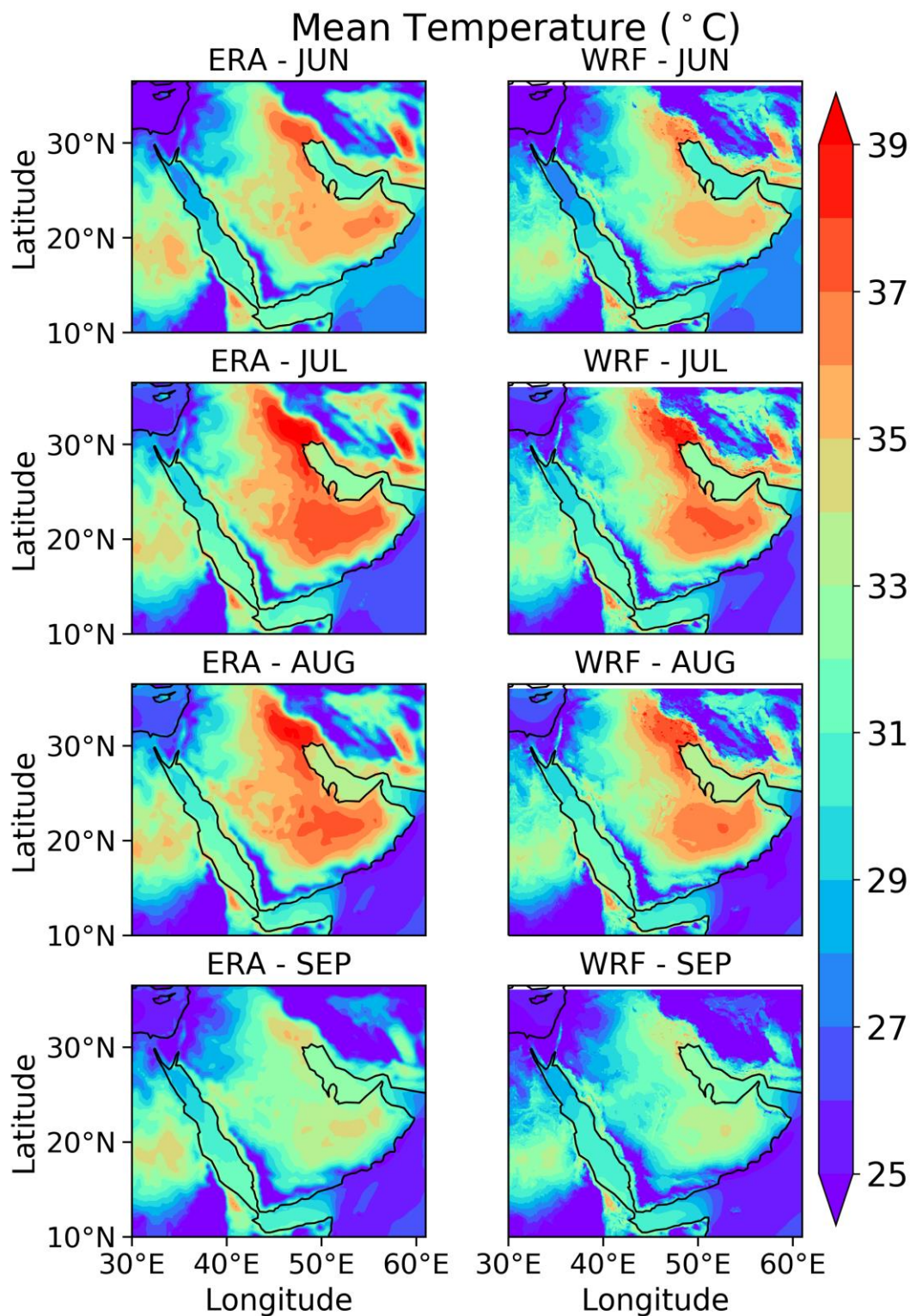


Figure 1. Mean monthly surface temperatures (°C) across the Kingdom of Saudi Arabia (KSA) from ERA and regional Arabian Peninsula (AP) reanalysis for June, July, August, and September.

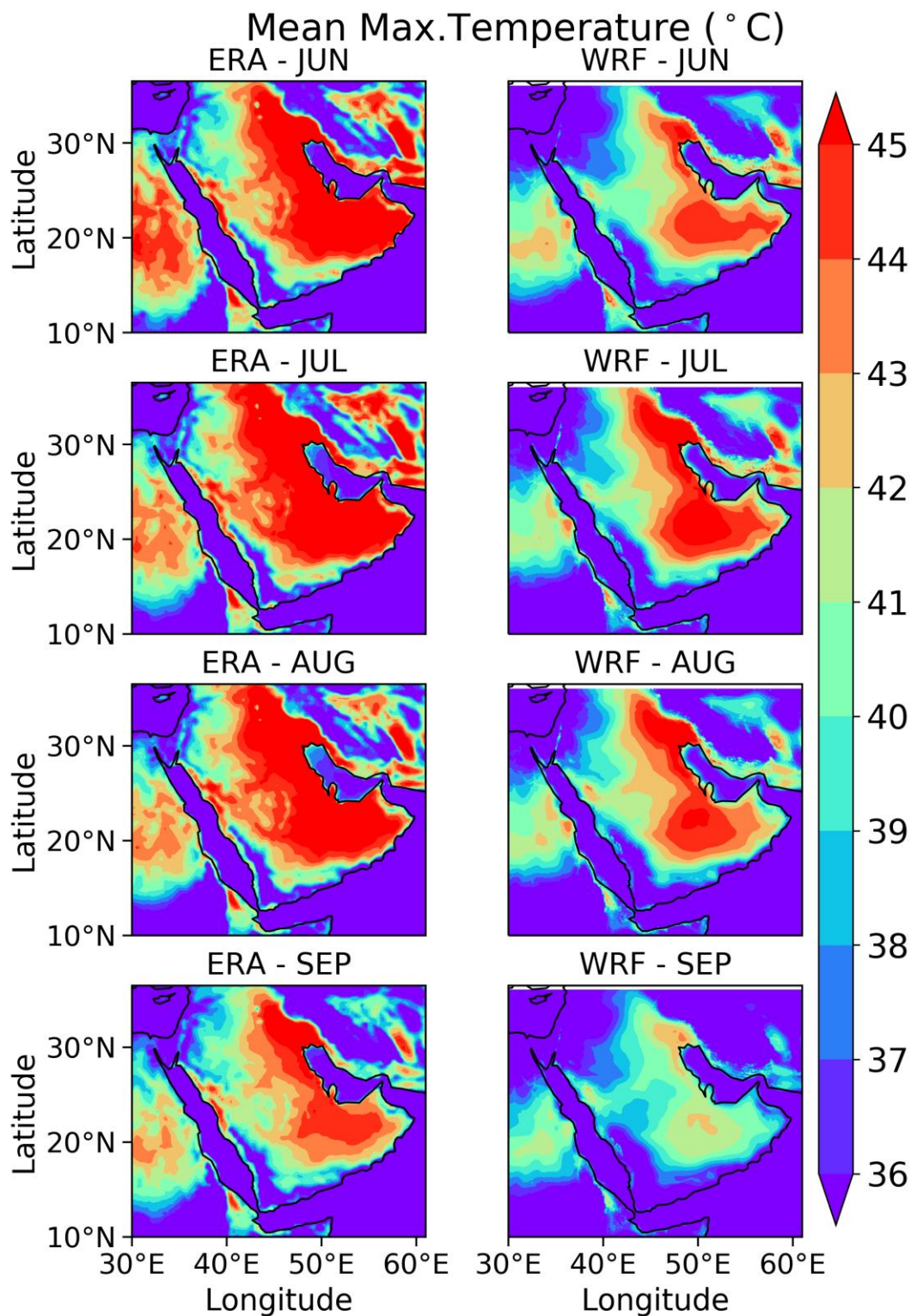


Figure 2. Mean monthly surface maximum temperatures (°C) across the KSA from ERA and regional AP reanalysis for June, July, August, and September.

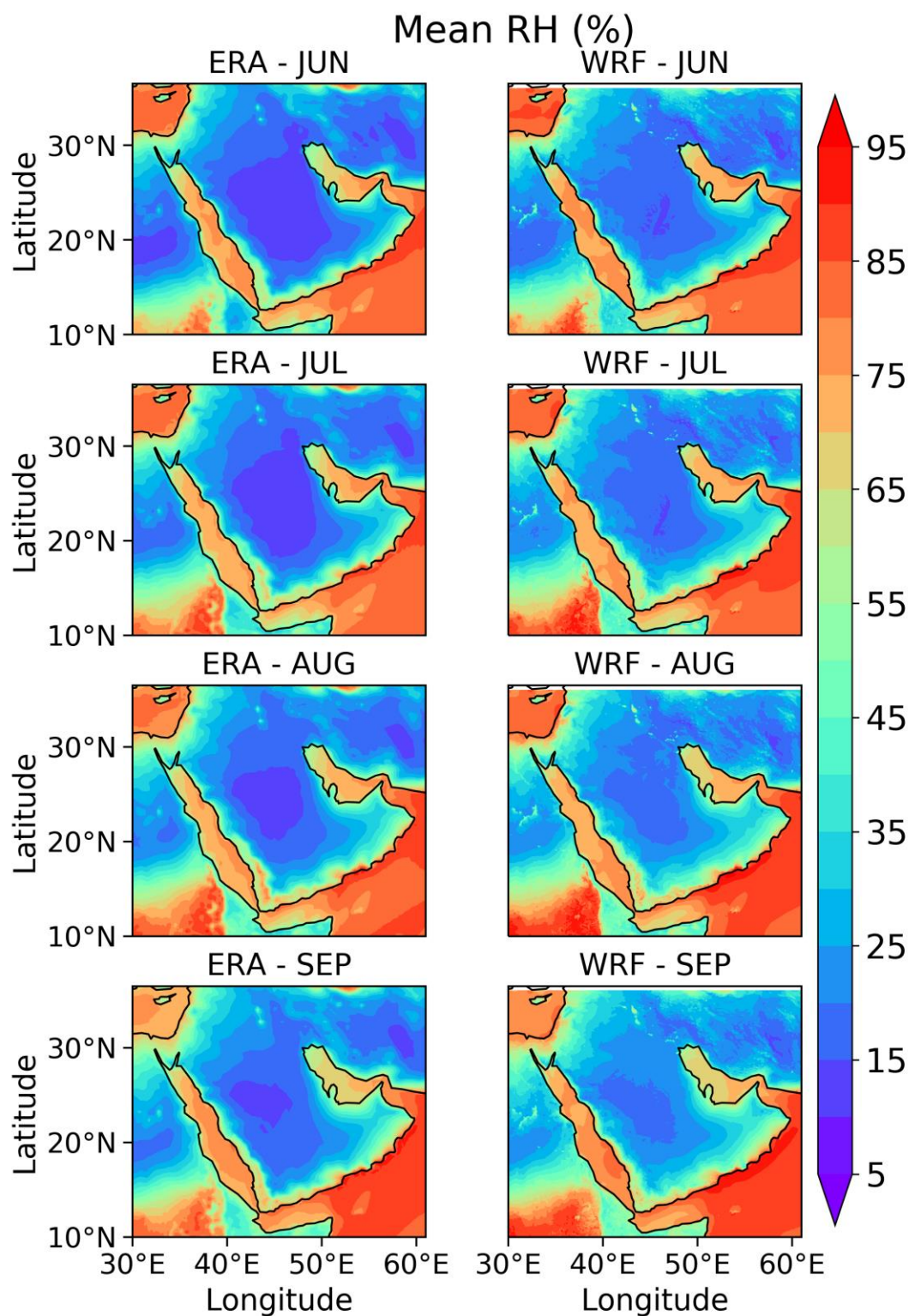


Figure 3. Mean monthly relative humidity (%) across the KSA from ERA and regional AP reanalysis for June, July, August, and September.

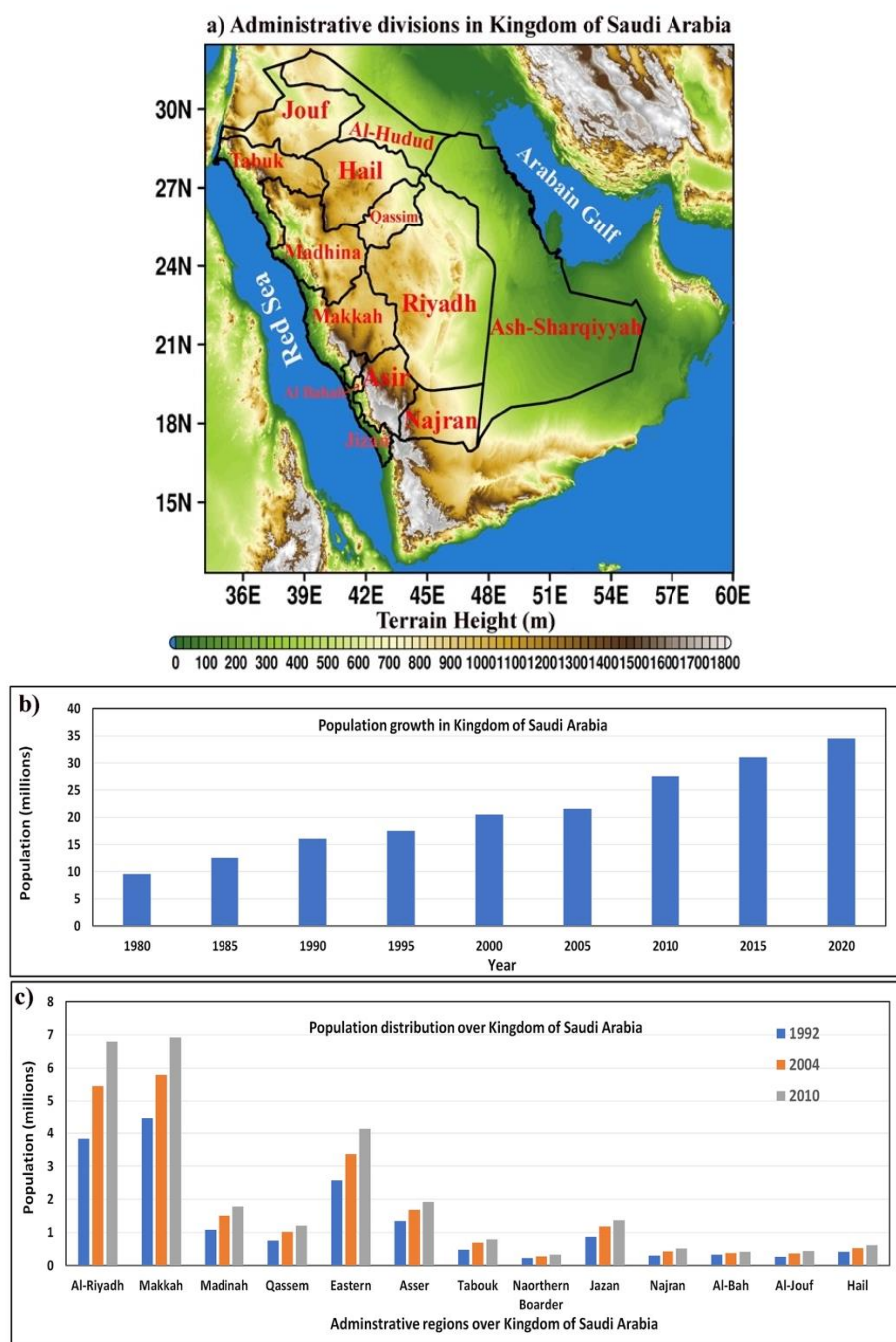


Figure 4. Population distribution across the Kingdom of Saudi Arabia (KSA). (a) administrative regions of the KSA, (b) population changes in the KSA, and (c) population in the different administrative regions in 1992, 2004, and 2010.

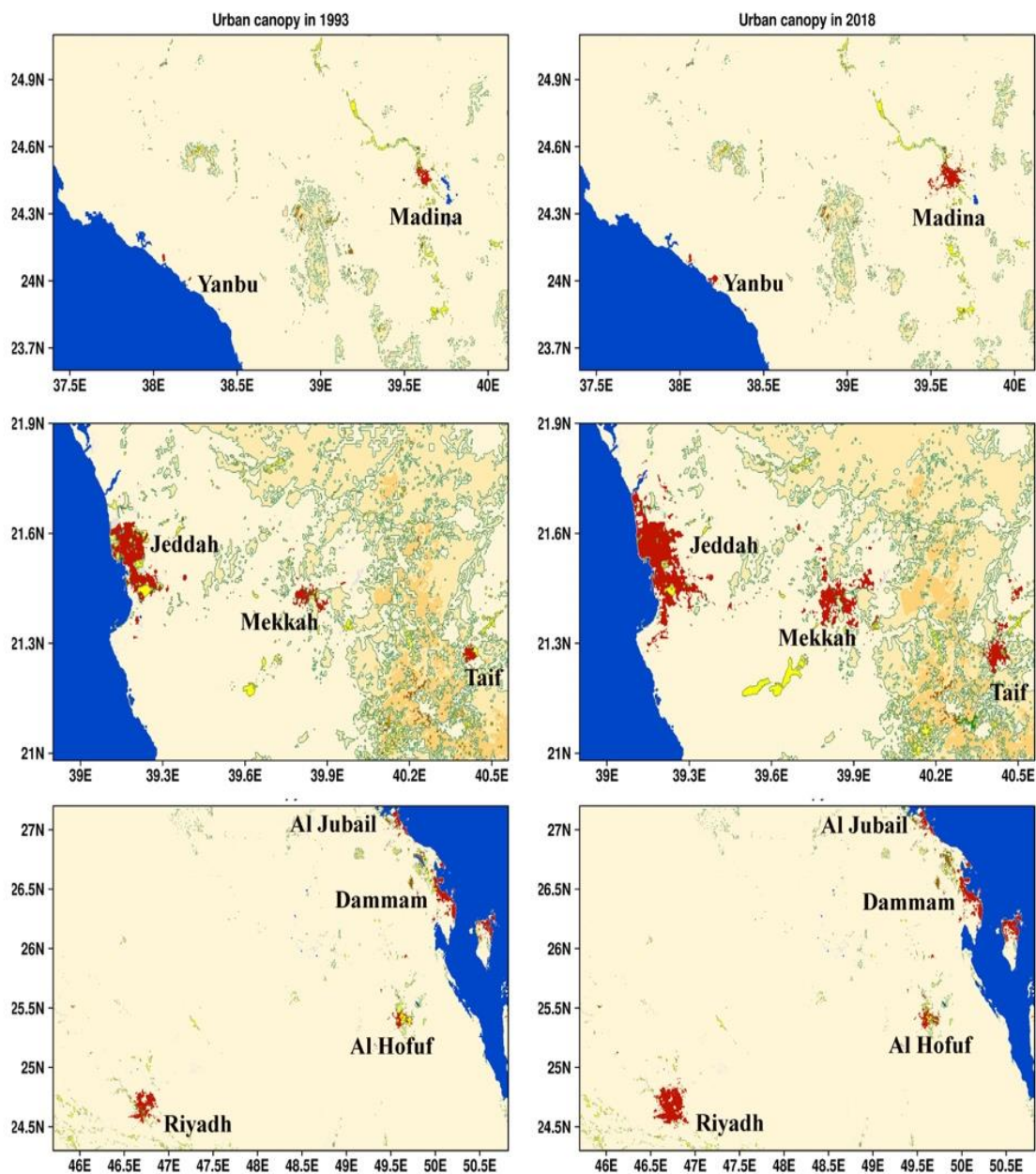


Figure 5. Changes in urban canopy (shown in red color) in various regions of the KSA. The left and right panels show data for the years 1993 and 2018, respectively.

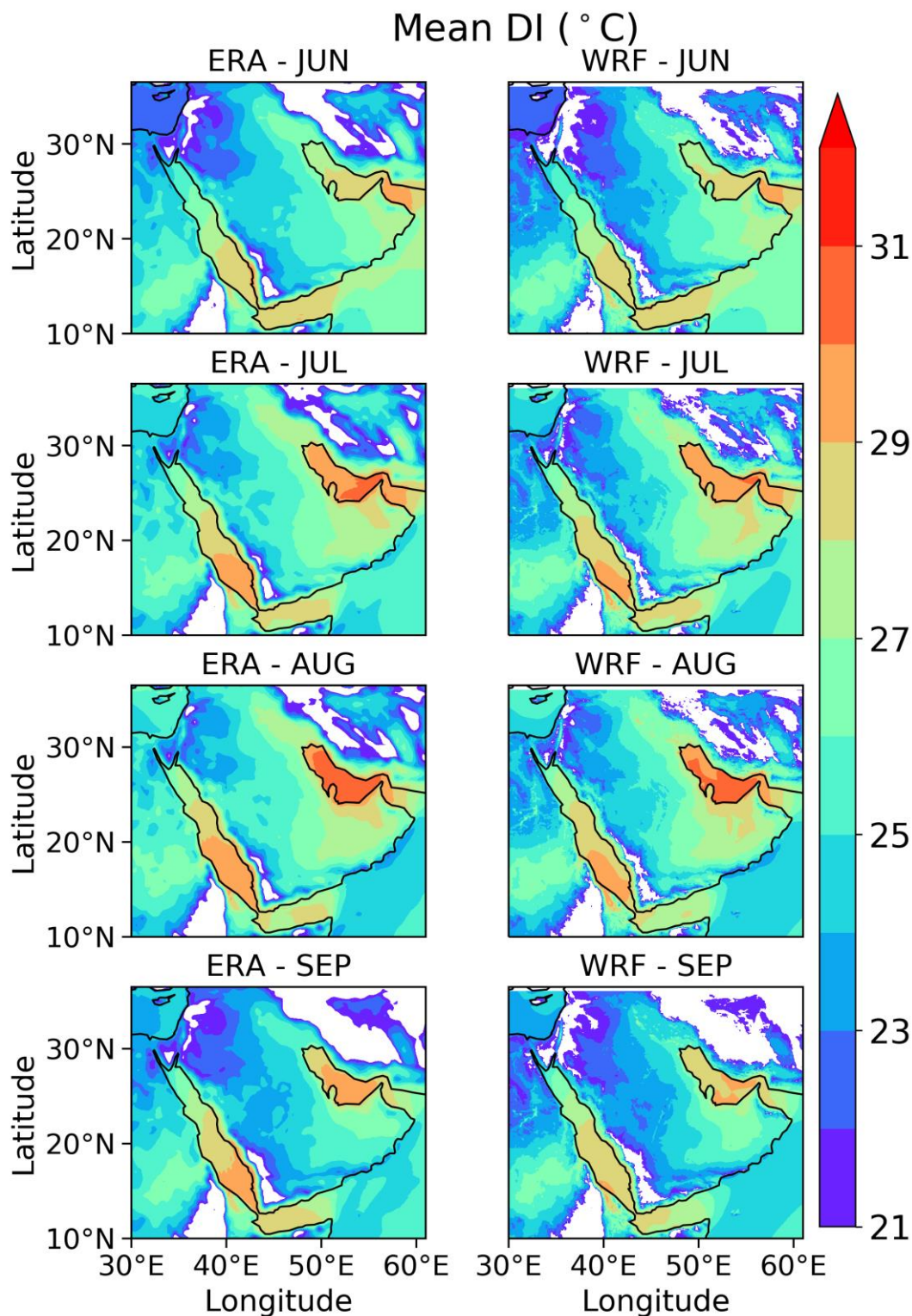


Figure 6. Mean monthly discomfort index (°C) across the KSA from ERA and regional AP reanalysis for June, July, August, and September.

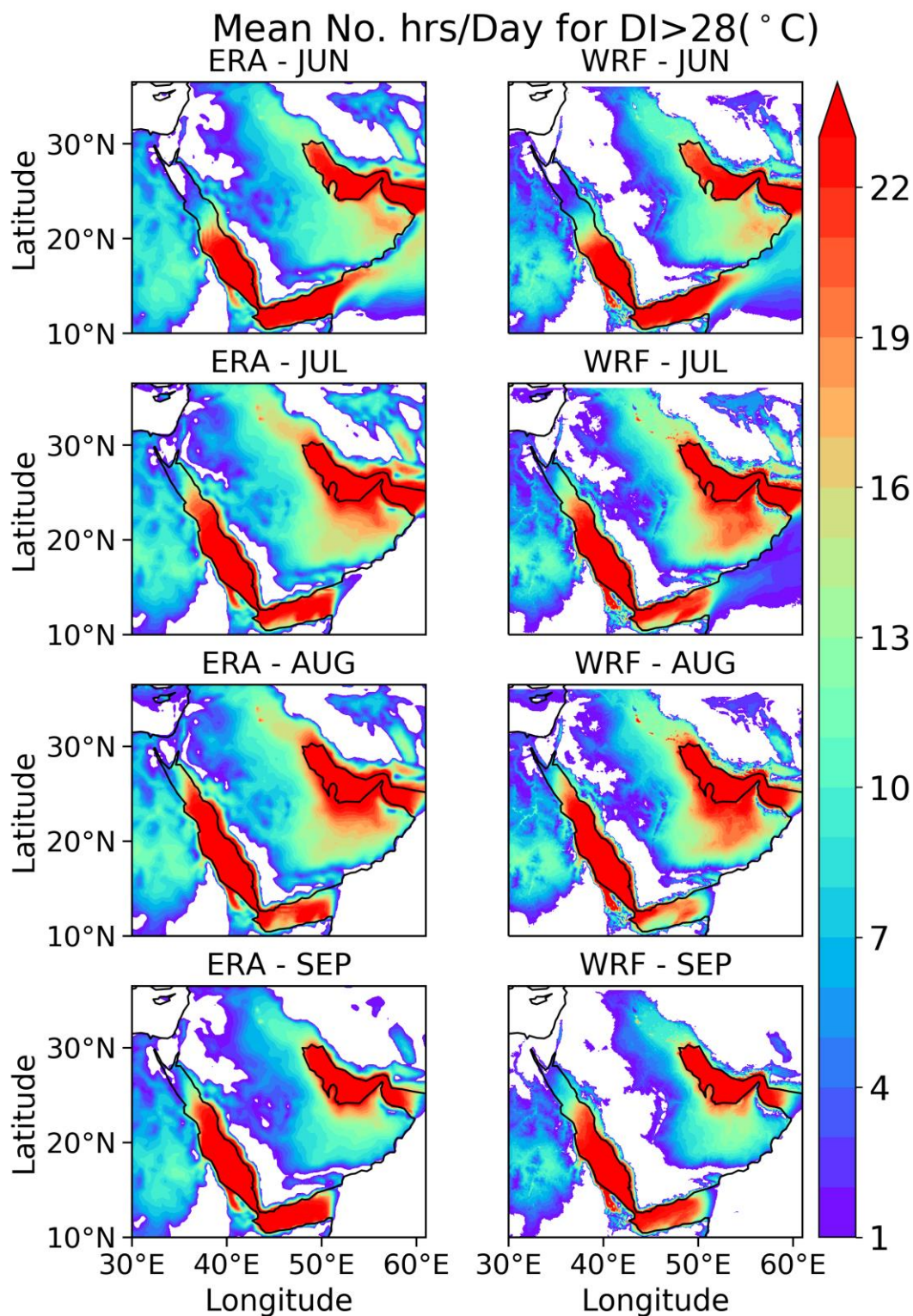


Figure 7. Mean number of hours per day with a discomfort index (DI) greater than  $28^{\circ}C$  across the KSA from ERA and regional AP reanalysis for June, July, August, and September.

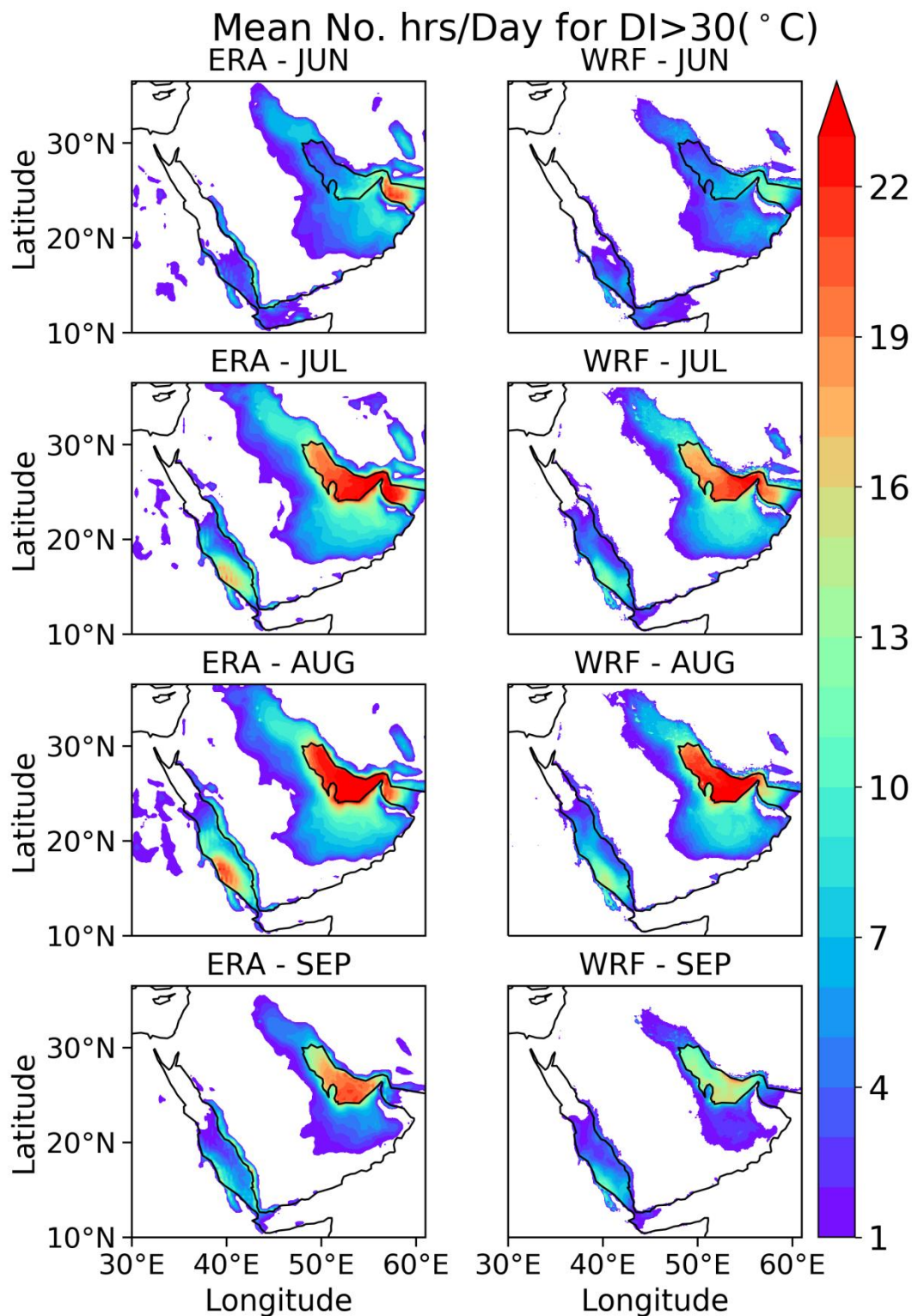


Figure 8. Mean number of hours per day with a discomfort index (DI) greater than  $30^{\circ}C$  across the KSA from ERA and regional AP reanalysis for June, July, August, and September.

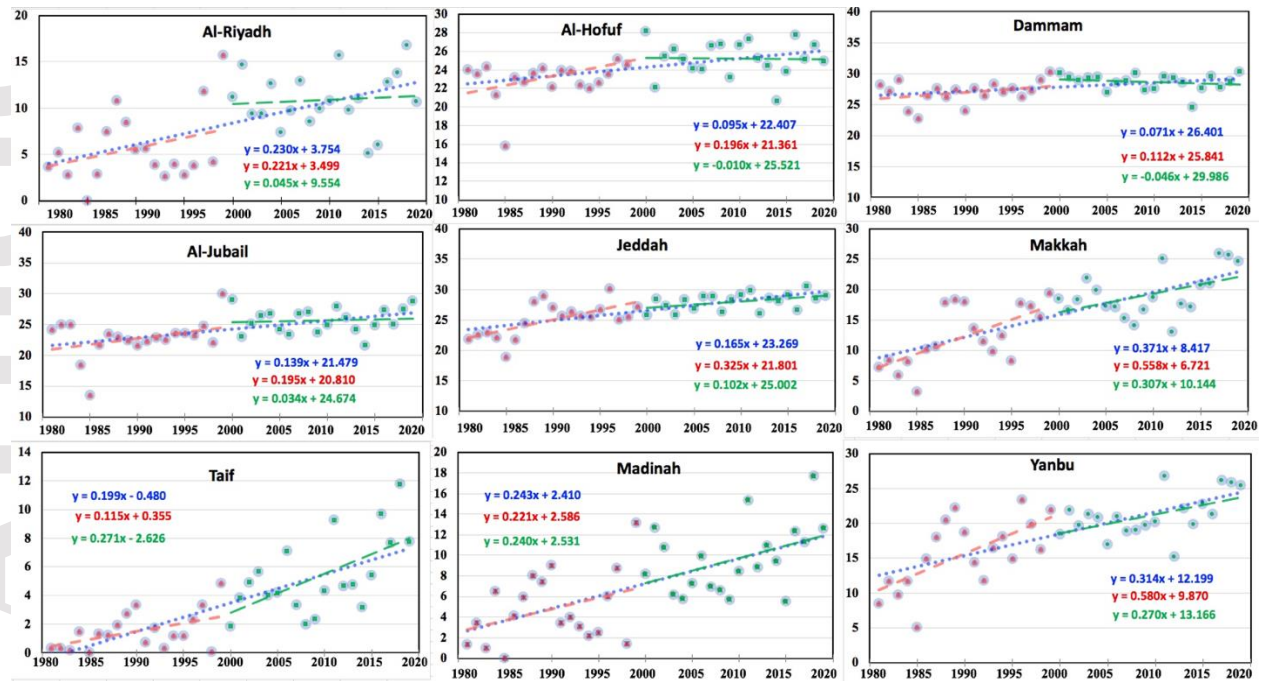


Figure 9. Long-term trends in the mean number of days in summer with a DI greater than 28°C persisting for 4–6 hours/day over the study period (1980–2018, blue), the first two decades (1980–1998, red), and the last two decades (1999–2018, green) in the major cities of the KSA.